J. Am. Chem. Soc. 1984, 106, 8014-8017

# EPR Study of the Chloroperoxy Radical, ClOO, Stabilized in the Zeolitic Host Matrix of Cancrinite

**P. Raghunathan* and S. K. Sur**

*Contribution from the Department of Chemistry, Indian Institute of Technology, Kanpur 208 016, India.* *Received February 14, 1984*

**Abstract:** Stabilization of the chloroperoxy radical, ClOO, produced by UV photoisomerizing chlorine dioxide (OClO) sorbed in the aluminosilicate host matrix of cancrinite at 77 K is reported, and a complete interpretation of the electron paramagnetic resonance (EPR) spectrum of ClOO is given. Analysis of the g, hyperine (A), and quadrupole (Q) tensors of ClOO and the assignments of the magnitudes as well as signs of their respective components have been made by simulating the details of the well-resolved low-temperature spectral line shapes. The first successful observation of the isotropic EPR spectrum of ClOO ($g_{iso} = 2.0015$, $A_{iso}(^{35}Cl) = 8.6 \times 10^{-4}$ cm$^{-1}$), observed upon allowing the matrix to warm up to 200 K, is also reported, and the electronic ground state of the radical is inferred to be of $^2A''$ symmetry. Good agreement is demonstrated between the experimental quadrupole interaction parameters for ClOO and corresponding estimates based on semiempirical MO calculations. A mechanism is discussed for the formation of ClOO in the cancrinite host.

The increasing use of zeolitic framework structures for free-radical entrapment in recent years has enabled not only the isolation of important free radical species but also the extensive characterization of their electron paramagnetic resonance (EPR) parameters.[1-3] We have recently demonstrated the usefulness of cancrinite, $Na_6[(AlO_2)_6(SiO_2)_6]$, a typical member of the felspathoid family in zeolite chemistry, as an efficient host matrix for a variety of radical species.[4,5] The framework structure of cancrinite belongs to the hexagonal space group $P6_3$ ($a = 12.7$ Å, $c = 5.1$ Å)[6,7] and has tubular channels parallel to its $c$ axis as well as smaller 11-hedral cages having "molecular" free dimensions, i.e., about 4.7 Å along the $c$ axis and 3.5 Å in the perpendicular direction. Since $CaCO_3$ is present in cancrinite as an "occluded salt" which blocks off diffusion pathways via the tubular channels, radical entrapment would be expected to be especially efficient in the cages.

The present work is an EPR study of the UV-induced photoisomerization of paramagnetic chlorine dioxide, OClO, to the chloroperoxy radical, ClOO, in the cancrinite matrix. Postulated as an important intermediate in early photolysis experiments of $Cl_2$ and $O_2$ gas mixtures[8] and also in gas-phase mechanisms concerning halogen monoxide formation,[9,10] the ClOO photoisomer has been observed only at low temperatures in rare gas matrices by infrared[11,12] and EPR[13,14] spectroscopic techniques; EPR spectra attributable to trapped ClOO have been reported also in irradiated potassium perchlorate at low temperatures.[15,16]

In the early EPR studies a substantial chlorine nuclear quadrupole interaction was found to complicate the spectral analysis. A further issue not heretofore settled is the electronic ground state of ClOO. The molecule belongs to the $C_s$ point group by virtue of having only a plane of symmetry, and may be classified as a "$\pi$"- or "$\sigma$"-radical depending on whether the unpaired electron is in an orbital of $^2A''$ symmetry or $^2A'$ symmetry, respectively. The previous EPR studies could not settle this point owing to the nonobservability of the *isotropic* $g$ value and chlorine hyperfine splitting constant. We have exploited the trapping efficiency of cancrinite to obtain not only a well-resolved low-temperature anisotropic spectrum of motionally rigid ClOO but also the motionally averaged isotropic spectrum that results at higher temperature.

## Experimental Section

Gaseous chlorine dioxide was prepared by the customary procedure[17,18] of slowly heating a mixture of oxalic acid and potassium chlorate in a chilled sulfuric acid solution. The evolved OClO was purified by drying over $P_2O_5$, pumped at 195 K to remove $CO_2$, and then trap-to-trap distilled from 195 to 77 K. Much cation was exercised in handling OClO as it is explosive. The gas was sorbed into powdered, "activated" synthetic cancrinite.[4b,19] On the basis of maximum signal intensity and EPR signal resolution, an optimum sorption pressure of $10^{-4}$ torr of OClO was established. Well-resolved EPR spectra were obtained after sorbing at the above pressure for about 15 min at 77 K. The EPR measurements were made on a Varian E 109 X-band spectrometer equipped with 100-kHz magnetic field modulation and low-temperature accessories. The frequency of the microwave radiation was measured with a Hewlett-Packard X 532B frequency meter, and the magnetic field with an Alpha 3093 digital NMR gaussmeter.

Ultraviolet irradiation of the OClO in cancrinite at 77 K was done with a Hanovia 100-W high-pressure mercury lamp equipped with a monochromator which selected the intense irradiation lines at 4350 Å where the absorption edge of OClO lies.

Our analysis of the molecular Zeeman, hyperfine, and quadrupole tensors (g, A and Q, respectively) was done by fitting computer-simulated line shapes to the experimental spectra. The line-shape simulation procedure, which was carried out on a DEC 1090 computer using a program we have developed[4b] based on Iwasaki's algorithm,[20] assumes a spin Hamiltonian of the form

$$\mathcal{H}_S = \beta_e H\cdot \mathbf{g}\cdot S + I\cdot \mathbf{A}\cdot S + I\cdot \mathbf{Q}\cdot I - g_n\beta_n I\cdot H \qquad (1)$$

---

[1] Kasai, P. H.; Bishop, R. J. Jr., "Zeolite Chemistry and Catalysis"; Rabo, J. A.; Ed.; American Chemical Society: Washington, DC, 1976; ACS Monogr. No. 171, Chapter 6, p 350.

[2] Che, M. "Magentic Resonance in Colloid and Interface Science"; Fraissard, J. P., Resing, H. A., Eds.; Reidel: Holland, 1980; p 79.

[3] Atanasova, V. D.; Kazanskii, V. B. *Russ. Chem. Rev.* (*Engl. Trans.*) **1981**, *50*, 209.

[4] (a) Raghunathan, P. *Proc. Int. Symp. Magn. Reson. Inorg. Mater.*; *Dushanbe* (*USSR*) **1982**; p 131. (b) Sur, S. K. Ph.D. Dissertation, Indian Institute of Technology, Kanpur, India, 1982.

[5] Raghunathan, P.; Sur, S. K. *J. Phys. Chem.* **1983**, *87*, 3383; *Proc. Ind. Acad. Sci.* **1983**, *92*, 597.

[6] Zarchow, O. *Z. Kristallogr.* **1965**, *122*, 407.

[7] Smith, J. V. In ref 1, Chapter 1, p 3.

[8] Porter, G. *Discuss. Faraday Soc.* **1950**, *9*, 60. Porter, G.; Wright, F. J. *Ibid.* **1953**, *14*, 23.

[9] Benson, S. W.; Buss, J. H. *J. Chem. Phys.* **1957**, *27*, 1382. Benson, S. W.; Anderson, K. H. *Ibid.* **1959**, *31*, 1082.

[10] Burns, G.; Norrish, R. G. W. *Proc. R. Soc. London Ser. A* **1963**, *271*, 289.

[11] Rochkind, M. M.; Pimentel, G. C. *J. Chem. Phys.* **1967**, *46*, 4481.

[12] Arkell, A.; Schwager, I. *J. Am. Chem. Soc.* **1967**, *89*, 5999.

[13] McDowell, C. A.; Nakajima, H.; Raghunathan, P.; Tait, J. C. *Proc. Colloq. AMPERE* **1968**, *15*, 345.

[14] Adrian, F. J.; Cochran, E. L.; Bowers, V. A. *J. Chem. Phys.* **1972**, *56*, 6251.

[15] Byberg, J. L. *J. Chem. Phys.* **1967**, *47*, 861.

[16] Eachus, R. S.; Edwards, P. R.; Subramanian, S.; Symons, M. C. R. *J. Chem. Soc. A* **1968**, 1704.

[17] Brauer, G. "Handbook of Preparative Inorganic Chemistry"; Academic Press: New York, 1963; Vol. 1, p 301.

[18] McDowell, C. A.; Raghunathan, P.; Tait, J. C. *J. Chem. Phys.* **1973**, *59*, 5858.

[19] Barrer, R. M.; Cole, J. F.; Sticher, H. *J. Chem. Soc. A* **1968**, 2475.

[20] Iwasaki, M. *J. Magn. Reson.* **1974**, *16*, 417.

0002-7863/84/1506-8014$01.50/0

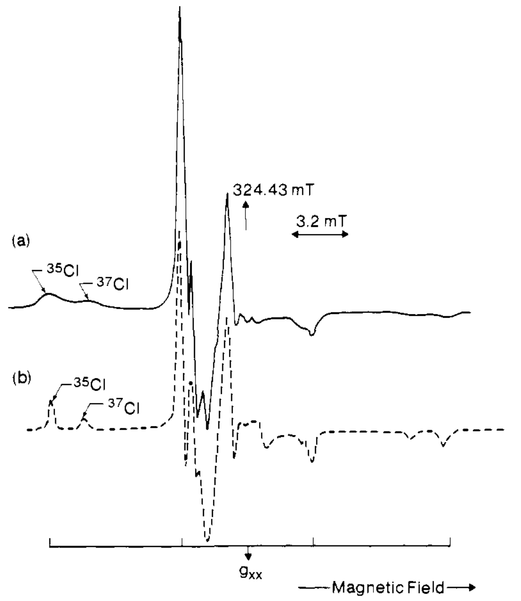

**Figure 1.** EPR spectrum of OClO sorbed in polycrystalline cancrinite at 77 K; (a) experimental, (b) computer simulated.

where $S$ and $I$ are the electron spin and nuclear spin vectors. $\beta_e$, $\beta_n$, and H are respectively the Bohr magneton, nuclear magneton, and the applied magnetic field, and $g_n$ is the nuclear $g$ factor. The resonance field positions calculated by eq 1 are convoluted with a Gaussian line-shape function with a peak-to-peak derivative line width appropriate to the spectrum being simulated.

The measured **g** values are accurate to ±0.0001 and the hyperfine splittings are accurate to $\pm 9.3 \times 10^{-6}$ cm$^{-1}$ (or 0.01 mT in magnetic field units).

## Results

**Entrapment of OClO in Cancrinite.** The successful trapping of OClO in the rigid matrix structure of cancrinite at 77 K has been confirmed by observing the development of its familar EPR spectrum.[18,21] A typical spectrum is shown by the solid line of Figure 1. The spectrum is sufficiently well resolved for the major hyperfine splittings from the $^{35}$Cl and $^{37}$Cl nuclear isotopes of spin $I = {}^3/_2$ to be distinguished and clearly exhibits characteristic anisotropies in both **g**- and hyperfine-tensor components. Guided by the earlier studies[18,21] we have verified by a computer simulation that the EPR parameters for OClO correspond to $g_{xx} = 2.0022$, $g_{yy} = 2.0133$, $g_{zz} = 2.0144$, $A_{xx}(^{35}\mathrm{Cl}) = 0.007\,201$ cm$^{-1}$, $A_{yy}(^{35}\mathrm{Cl}) = 0.001\,681$ cm$^{-1}$, and $A_{zz}(^{35}\mathrm{Cl}) = 0.000\,747$ cm$^{-1}$. The "best fitting" computed line shape is shown as the dotted line in Figure 1.

**Formation and Entrapment of ClOO in Cancrinite.** After about 20 min of UV irradiation of the OClO in cancrinite at 77 K a sudden decrease in the EPR absorption intensity of OClO (Figure 1) was observed, along with the eventual buildup of the isomeric species, as revealed by its well-resolved EPR spectrum (solid line, Figure 2a). Once again, hyperfine splittings from both chlorine isotopes are discernible, and the spectrum is typical of a radical possessing an anisotropic **g** tensor and a small but highly anisotropic hyperfine coupling tensor. Further analysis of the line shapes of Figure 2 is carried out in the next section.

The cancrinite sample was then allowed to warm up slowly while continuously monitoring the signals, with a view to recording the isotropic spectrum of ClOO. A gradual transition was seen to occur, the anisotropic spectrum displayed in Figure 2 slowly changing into a much simpler four-line spectrum. The isotropic spectrum shown in Figure 3 is the one recorded at 200 K. Above this temperature the intensity of the signal decreased, possibly because of diffusion of ClOO.

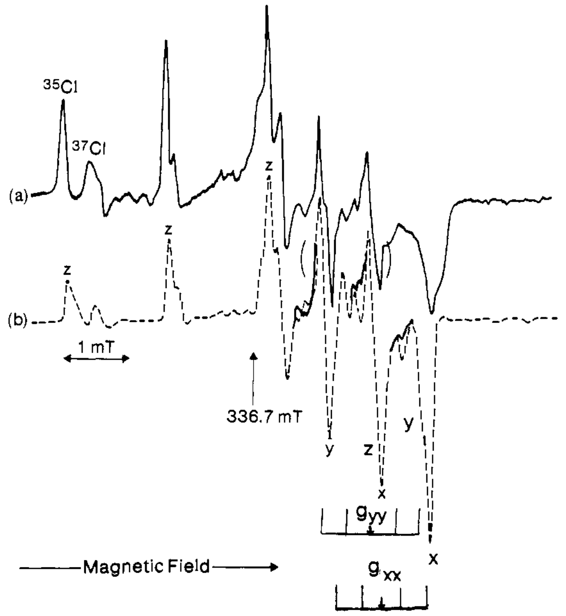

**Figure 2.** EPR spectrum of ClOO produced in cancrinite at 77 K: (a) experimental, (b) computer simulated. Details of the dotted and solid lines inside the bracketed region are discussed in the text. The stick pattern indicates allowed $x$ and $y$ transitions.

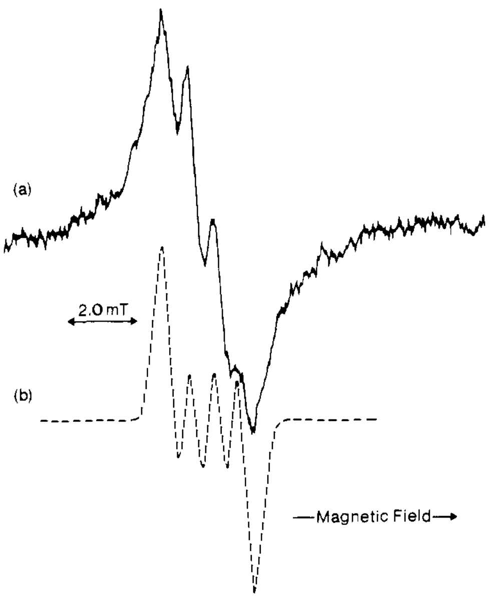

**Figure 3.** Isotropic EPR spectrum of ClOO in cancrinite at ~200 K: (a) experimental, (b) computer simulated.

Our line-shape simulation of the isotropic spectrum, computed for $A_{iso}(^{35}\mathrm{Cl}) = 8.6 \times 10^{-4}$ cm$^{-1}$ and $g_{iso} = 2.0015$ as the "best-fit" values, is displayed as the dotted curve of Figure 3. In the next section, the above experimental results are discussed and the EPR parameters as well as the electronic ground state of ClOO established.

## Discussion

The gross features of the EPR spectrum of Figure 2 are readily identifiable as belonging to the chloroperoxy radical, measurements of the largest **g**- and hyperfine-tensor components agreeing particularly well with the earlier assignments.[13,14] However, the high-field portion of our spectrum is seen to be rich in better resolved details of a large quadrupole interaction. The Cl–O bond axis (Figure 4), chosen as the $z$ direction in our line-shape computations, should define the principal direction about which the quadrupole tensor should exhibit axial or near-axial symmetry. By adoption of the choice of principal axes described in Figure 4 and assumption that the principal directions of the **g**, **A**, and **Q**, tensors coincide, trial simulations of the EPR spectrum were performed for initial values of the tensor components. However,

---

(21) Coope, J. A. R.; Gardner, C. L.; McDowell, C. A.; Pelman, A. I. *Mol. Phys.* **1971**, *21*, 1043.

**Table I.** Experimental Principal Values of the Spin Hamiltonian Tensors for $^{35}$ClOO

| g tensor | | | | $^{35}$Cl hyperfine tensor, $10^4$ cm$^{-1}$ | | | | quadrupole tensor, $10^4$ cm$^{-1}$ | | |
|---|---|---|---|---|---|---|---|---|---|---|
| $g_{xx}$ | $g_{yy}$ | $g_{zz}$ | $g_0$ | $A_{xx}$ | $A_{yy}$ | $A_{zz}$ | $A_0$ | QD | QE | ref |
| 1.9981 | 1.9984 | 2.0079 | 2.0015 | −3.9 | −4.6 | −17.3 | \|8.6\| | −8.7 | 0.0 | this work |
| 1.9965 | 1.9987 | 2.0100 | | ∓4.3 | ∓1.9 | ∓16.8 | | ±6.8 | ±0.1 | 15 |
| 1.9983 | 2.0017 | 2.0130 | | \|4.9\| | \|6.7\| | \|14.0\| | | | | 16 |
| 1.9915 | 1.9987 | 2.0100 | | \|5.36\| | \|3.0\| | \|16.6\| | | −8.757 | | 14 |

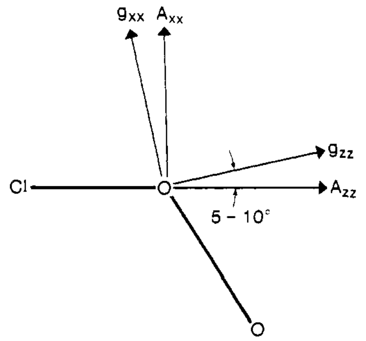

**Figure 4.** Principal axis system for ClOO; not shown is the out-of-plane $y$ axis.

the poor quality of the initial line-shape simulations led to the inference that the three principal tensors may not be coaxial. The hyperfine and quadrupole tensors would be expected to have their principal component axes parallel since they should both be dominated by the Cl–O bond. The **g** tensor, however, is likely to be governed more by the newly formed O–O bond, and hence one component of the tensor would be aligned along this bond. The Cl–O–O bond angle has been assessed reliably by IR analysis[12] to be 110°, which would suggest a value somewhere in the range 0–20° for the angle between the **g** and **A** or **Q** tensors in the molecular plane (by symmetry, the out-of-plane axes must be coincident).

A choice must now be made as to which tensor component ($x$ or $y$) is to be directed along the common axis. For each choice, line-shape simulations were run on the computer for various angles ($\theta$) between the in-plane **g** and **A** (or **Q**) tensor axes (up to a limit of 20°, as mentioned above). It was immediately apparent that when the **g** value component closest to the "free-spin" value of 2.0023 was directed along the common axis perpendicular to the molecular plane, quite reasonable simulations resulted when $\theta$ was within the 5–10° range and, above this range, pronounced discrepancies resulted between the experimental and computed line shapes. On the other hand, when this component was chosen to lie along the axis perpendicular to the Cl–O bond and *in* the Cl-O-O plane, substantial departures from the high field spectral intensities and line positions of the experimental spectrum were observed.

Further computations revealed that the positions and intensities of the high-field transitions were indeed sensitive to the $z$ component of the quadrupole tensor, QD. The dotted curve shown in Figure 2b, which is a close fit to the observed spectrum, has been obtained by solving eq 1 for $g_{xx} = 1.9981$, $g_{yy} = 1.9984$, $g_{zz} = 2.0079$, and the values (in units of $10^{-4}$ cm$^{-1}$) of $A_{xx} = 3.9$, $A_{yy} = 4.6$, and $A_{zz} = 17.3$, QD = −8.7, and convoluting the resultant line positions with a Gaussian shape function of width 0.0003 cm$^{-1}$. Some of the high-field features of Figure 2b shown within the bracketed region and the corresponding experimental spectrum are still somewhat mismatched. However, altering the signs of the hyperfine tensor components such as to render all of them negative resulted in the following: (a) the "allowed" line positions corresponding to the central $x$ and $y$ component transitions (marked "$x$" and "$y$" in Figure 2b) remained unshifted, although somewhat altered in intensity: (b) shifts were observed in the calculated line positions of the "forbidden" $\Delta m_I = \pm 1, \pm 2$ transitions indicated by solid lines in Figure 2b, and the intensities of these transitions were also seen to minimize the mismatch between the experimental and simulated line shapes. The overall refinements that resulted are distinguished by the solid line features of the dotted curve in Figure 2b. The spin Hamiltonian parameters appropriate to this simulation as well as the isotropic **g** and **A** values determined in the previous section are set forth in Table I, along with a comparisons of the results of earlier workers.

Were the peroxy radical to have a $^2$A″ ground state, then $\pi$-radical theory[22] predicts that the **g**-tensor component perpendicular to the molecular plane would be closest to the free-spin value; this direction would also define the largest component of the hyperfine coupling tensor. In other words, this component of **A** should come out orthogonal to QD which is along the bond direction. Our line-shape analysis has, however, led to an unambiguous assignment of the largest hyperfine interaction component, $A_{zz}$, *along* the Cl–O bond. To rationalize this assignment in a $\pi$-radical, a substantial spin polarization of this bond must be invoked,[23] whereby the Cl hyperfine-tensor becomes dominated by a negative spin density in the O–Cl $\sigma$-bond induced by a large positive spin density in the $p_\pi$ orbital of the central oxygen atom. In line with this mechanism, the only compatible choice of sign as well as axis in our assignment will lead to $A_{zz}$ being negative and the smallest hyperfine component being oriented along the $x$ axis. We could accordingly decompose the observed **A** tensor and get for the anisotropic (traceless) part the values (+4.7, +4.0, and −8.7) × $10^{-4}$ cm$^{-1}$ along the $x$, $y$, and z directions, respectively,

$$\mathbf{A} = \begin{pmatrix} A_{xx} & & \\ & A_{yy} & \\ & & A_{zz} \end{pmatrix} = \left[ -8.6 \begin{pmatrix} 1.0 & & \\ & 1.0 & \\ & & 1.0 \end{pmatrix} + \begin{pmatrix} +4.7 & & \\ & +4.0 & \\ & & -8.7 \end{pmatrix} \right] \times 10^{-4}\ \mathrm{cm}^{-1}$$

We note that this analysis requires the isotropic hyperfine splitting to be negative, −8.6 × $10^{-4}$ cm$^{-1}$. The magnitude of this value is in excellent agreement with the experimentally assessed isotropic hyperfine splitting.

The other alternative is to consider the $\sigma$ ($^2$A′) ground state for ClOO based on the decomposition of the experimental **A** tensor into an isotropic value of +8.6 × $10^{-4}$ cm$^{-1}$ and a traceless component of (−4.7, −4.0, +8.7) × $10^{-4}$ cm$^{-1}$. However, we have already shown that a spectral simulation based on **A** tensor values corresponding to this decomposition leads to a somewhat poorer agreement with the experimental line shapes. Further, in the $^2$A′ ground state the unpaired electron orbital would be composed primarily of p atomic orbitals directed perpendicular to the O–O bond so that $g_{zz}$ would be expected to be much closer to 2.0023 than has been determined experimentally. We rule out the $^2$A′ ground state for ClOO on the above grounds.

Although the values of all three **g** components are consistent with the $\pi$-radical symmetry proposed for ClOO, the following comments are in order. The small negative **g** shift of the component perpendicular to the molecular plane ($\Delta g_{yy} = g_{yy} - 2.0023 = -0.0039$) cannot be rationalized on the basis of one-center **g**-tensor theory for a $\pi$-radical[22] and it would seem necessary to consider nonnegligible contributions from two-center terms. $\Delta g_{xx}$ is also small and negative; as postulated by Adrian[23] for FOO, this shift may be understood as being the net result of two spin orbitally coupled excitations which yield **g** shifts of opposite sign, one of which involves a transition from a filled low-lying $\sigma$ MO to the unpaired electron $\pi$ MO and the other involves a transition from the unpaired electron orbital to a slightly higher $\sigma^*$ orbital.

---

(22) McConnell, H. M.; Robertson, R. E. *J. Phys. Chem.* **1957**, *61*, 1018.
(23) Adrian, F. *J. Chem. Phys.* **1967**, *46*, 1543.

**Table II.** Nuclear Quadrupole Coupling Data for $^{35}ClOO$

| nuclear quadrupole coupling constant, MHz | quadrupole tensor, $\times 10^4$ cm$^{-1}$ | | ref | remark |
|---|---|---|---|---|
| | QD | QE | | |
| 109.746 | | | 23 | from atomic spectra |
| 105.000 | −8.757 | | 14 | from ClOO in Ar matrix |
| 81.000 | −6.755 | −0.1 | 15 | from ClOO in irradiated $KClO_4$ cyrstal |
| 104.052 | −8.70 | | this work | from ClOO in cancrinite |
| 102.816 | −8.575 | ~0.0 | this work | from SCF-MO-CNDO/2 calculation |

We have also checked the experimental quadrupole tensor components for ClOO by a semiempirical LCAO-MO calculation. Recalling that the quadrupole coupling constant, $q$, of a nucleus measures the interaction of the nuclear quadrupole moment ($Q$) with the electric field gradient (efg) tensor representing the external electric charge distribution, we write the efg matrix at the chlorine nucleus as[24]

$$(q_{Cl})_{ij} = \langle i | 3(\cos^2 \phi) - 1/r^3 | j \rangle \qquad (2)$$

where $|i\rangle$ and $|j\rangle$ are the appropriate MO states of electrons $i$ and $j$, r the nucleus–electron vector, and $\phi$ the angle the principal axis of the efg makes with r. On the other hand, the efg per unit charge of a nucleus, say, O of ClOO at the Cl nucleus will be given by

$$q_{Cl\text{-}O} = (3(\cos^2 \phi_{Cl\text{-}O}) - 1)/R_{Cl\text{-}O}^3 \qquad (3)$$

where $R_{Cl\text{-}O}$ is the Cl–O bond distance and $\phi_{Cl\text{-}O}$ the angle the efg makes with the bond direction. In principle, computation of the efg according to eq 2 necessitates the handling of tedious three-center integrals. Nevertheless, simplified efg calculations using one-center integrals only are feasible in terms of the well-known Townes–Dailey[25] approximations, and in our work we have used these approximations, which have been adapted for the LCAO-MO formulation by Sichel and Whitehead.[26]

In Table II our quadrupole coupling data are compared with those of previouis workers.[14,15] The asymmetry parameter has been found to be vanishingly small, thus supporting our previous conclusion regarding a negligible QE term. The calculated quadrupole coupling constant, $-8.575 \times 10^{-4}$ cm$^{-1}$, is in excellent agreement with the corresponding experimental value (QD = $-8.70 \times 10^{-4}$ cm$^{-1}$). Our calculation also predicts a shift of about 2° of the $z$ principal component of the efg from that of the Cl–O bond direction. This value, although small, does support the axis alignment necessary for the line-shape simulation discussed earlier, i.e., the shift of the **Q**-tensor axes by about 5–10° from the **g**-tensor axes (see Figure 4).

Regarding the mechanism of formation of ClOO from the symmetrical OClO in matrices, Arkell and Schwager[12] have proposed that the first step involves the formation of a partial O–O bond and a compressed Cl–O–O bond angle. Even a slight rotation of the molecule in the cage would allow the bond angle to increase to attain a more stable structure in the matrix. This radical isomerization is likely to be enhanced by the caging efficiency of the host matrix, which would restrict all three atoms to a confined space such as exists, for example, in a cancrinite cage,[7]

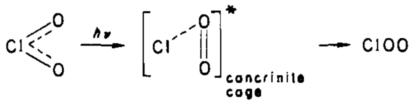

The above process most likely involves the intermediacy of an excited state of OClO and, since a relatively small photochemical energy is involved in the conversion, the excited state lies very close to the ground state of OClO. It has been observed in γ-irradiated crystalline $KClO_4$[15] that the ClOO radical is formed with about 75% yield when the initially formed OClO is UV irradiated and that if the crystal is allowed to stand at 295 K rapid reversion to OClO occurs with about 70% yield. This result implies that OClO is thermodynamically the stabler isomer and that the barrier to interconversion is small in $KClO_4$, whereas evidently the ClOO is stabilized to a somewhat larger extent in cancrinite.

## Conclusion

The photochemical production and stabilization of ClOO in cancrinite host matrix at 77 K is demonstrated by EPR spectroscopy. The isotropic EPR spectrum of ClOO has been obtained for the first time by allowing the matrix to warm up to 200 K. A unique assignment of the complete **g**, **A**, and **Q** tensors of ClOO, as well as the signs of the components of **A** and **Q** along the respective molecular axes, has been made by analyzing the EPR line shapes. The experimental quadrupole interaction parameters evaluated for ClOO are seen to compare favorably with those obtained by semiempirical MO calculations. The mechanism of formation of ClOO in the cancrinite cage is discussed.

A further important conclusions is that ClOO stabilized in cancrinite has a $^2A''$ ground electronic state. From the theoretical standpoint the possibility of a σ ground state for ClOO has been considered in a couple of quantum chemical studies,[27,28] although difficulties were often encountered in handling the near degeneracy of the filled valence orbitals of ClOO. We note that the geometry of the π-radical ($^2A''$ symmetry) structure for ClOO optimized in a recent ab initio SCF-MO calculation[29] leads to a Cl–O–O angle of 115°, which compares well with the shapes rationalized for the radical in the present and earlier[12] studies. We add here that a series of recent ab initio calculations[30] at the RHF-SCF level using 6-31G basis orbitals and 6-31G+ polarization functions, with complete optimization of geometry and including configuration interactions, indicate a $^2A''$ ground state with a close-lying upper state of $^2A''$ symmetry for ClOO.

**Acknowledgment.** The manuscript was completed while P.R. was a Visiting Professor at the Department of Chemistry, University of Alberta, Edmonton, Canada, and he wishes to thank Professor Otto Strausz for his hospitality during that time. Several important comments by three referees have led to the refinements in the line-shape simulation discussed in the text.

**Registry No.** ClOO, 93085-22-4; OClO, 10049-04-4; cancrinite, 12172-98-4.

---

[24] Lucken, E. A. C. "Nuclear Quadrupole Coupling Constants"; Academic Press: New York, 1969, p 121.

[25] Townes, C. H.; Dailey, B. P. *J. Chem. Phys.* **1949**, *17*, 782.

[26] Sichel, J. M.; Whitehad, M. A. *Theor. Chim. Acta* **1968**, *11*, 263.

[27] Gole, J. L.; Hayes, E. F. *Int. J. Quant. Chem.* **1970**, *3S*, 519.

[28] Farantos, S.; Leisegang, E. C.; Murrell, J. N.; Sorbie, J. J.; Texeira-Dias, C.; Varandas, A. J. C. *Mol. Phys.* **1977**, *34*, 947.

[29] Hinchliffe, A. *J. Mol. Struct.* **1980**, *64*, 117.

[30] Gosavi, R. K.; Raghunathan, P.; Strausz, O. P., unpublished results.